Progress In Electromagnetics Research, Vol. 108, 361–383, 2010

THEORETICAL ESTABLISHMENT AND EVALUATION OF A NOVEL OPTIMAL PYRAMIDAL HORN DESIGN CRITERION

K. B. Baltzis

RadioCommunications Laboratory
Section of Applied and Environmental Physics
Department of Physics
Aristotle University of Thessaloniki
Thessaloniki 541 24, Greece

Abstract—This paper proposes a novel design criterion for optimal pyramidal horns. According to the criterion, the optimal aperture phase error parameters of a pyramidal horn are determined from the minimization of the horn's lateral surface area. We present two families of curves that illustrate the optimal aperture phase error parameters for frequency and directivity values in the area of practical interest. We also discuss two simple approximate design methods for the calculation of the optimal horn parameters. Comparisons with well-known design methods demonstrate the efficacy of our approach. The designed horns have also smaller aperture area and require less installation space than other optimal proposals in the published literature. Moreover, the proposed criterion produces, under certain conditions, the lightest horn for a given directivity; as a result its fabrication requires less material compared to other structures. The present approach is a useful design tool when the size and weight of a pyramidal horn are of concern.

1. INTRODUCTION

Microwave horn antennas occur in a variety of shapes and sizes and are used in areas such as wireless communications, electromagnetic sensing, nondestructive testing and evaluation, radio frequency heating and biomedicine [1–10]. Horns are also widely used as high gain elements in phased arrays and as feed elements for reflectors and

Received 23 July 2010, Accepted 10 September 2010, Scheduled 28 September 2010
Corresponding author: K. B. Baltzis (kbaltzis@auth.gr).

lens antennas in satellite, microwave and millimeter wave systems. Moreover, they serve as a universal standard for calibration and gain measurements of other antennas.

The simplest and probably the most reliable horn antenna is the pyramidal horn. This is a hollow pipe of a rectangular or square cross section that flares to a larger opening. Its simplicity in construction, high gain, ease of excitation, robustness, versatility, linear polarization and unidirectional pattern makes it a useful tool in science and engineering.

This interest has resulted in a variety of proposals for the design of optimal pyramidal horns. The optimum gain pyramidal horn is commonly used [11–21]. In this, the aperture dimensions give maximum slant lengths of flare in the E- and H-planes [1]. Another optimal design criterion was proposed in [2]. It was observed that the gain increases with aperture width but the quadratic phase error loss increases faster and produces a maximum point. The maxima in the two principal planes occur at approximately constant phase deviations independent of the slant radius and define the optimal horn. In [22], the optimal pyramidal horn was defined as the horn that has approximately equal beamwidths in the E- and H-planes, while using the minimum material for its manufacturing. In that approach, the optimal aperture phase errors were specified graphically. In [23], horns design considered directivity and half-power beamwidths. The optimality was obtained by giving to one of the aperture phase error parameters its optimal value according to the optimum gain criterion while the rest of the parameters were derived to satisfy the constraints for the half-power beamwidths.

In this paper, we suggest a novel optimal pyramidal horn design criterion, the minimum lateral surface area (MLSA) criterion. According to it, the optimal pyramidal horn's dimensions are found from the minimization of its lateral surface area. The exact analytical calculation of the optimal dimensions of the horns is not possible. However, using curve-fitting analysis and interpolation techniques we obtain two simple design methods that allow the approximate but adequate design of optimal pyramidal horns with minimum lateral surface area. Comparisons with methods in the published literature demonstrate the efficacy of the approach.

The rest of the paper is organized as follows: Section 2 discusses some theoretical background. The proposed criterion is introduced in Section 3. Section 4 describes the two approximate design methods. In Section 5, representative examples and comparisons with well-known optimization criteria show the merits of the proposal. Finally, Section 6 concludes the paper.

2. PYRAMIDAL HORN GEOMETRY AND BASIC PRINCIPLES

Figure 1 shows the geometry of a pyramidal horn with throat-to-aperture length (axial length) P and aperture sizes A and B. The inner dimensions of the feeding rectangular waveguide are a and b. In our analysis, we assume that the horn is well-matched to the rectangular waveguide and operates in the dominant TE_{10} mode.

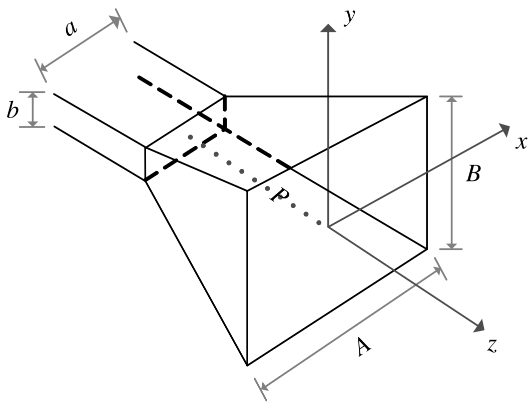

Figure 1. Geometry of a pyramidal horn antenna and coordinate system.

The directivity of the horn (in natural units) is [1, 2, 24]

$$D = \frac{32AB}{\pi\lambda^2} R_E R_H \tag{1}$$

where λ is the free-space wavelength. The factors R_E and R_H represent the reduction in gain due to the amplitude and phase taper across the horn aperture. They are calculated from [20, 23, 25]

$$R_E = \frac{C^2\left(2\sqrt{s}\right) + S^2\left(2\sqrt{s}\right)}{4s} \tag{2}$$

$$R_H = \frac{\pi^2}{64t}\left\{\left[C\left(\frac{1+8t}{4\sqrt{t}}\right) - C\left(\frac{1-8t}{4\sqrt{t}}\right)\right]^2 + \left[S\left(\frac{1+8t}{4\sqrt{t}}\right) - S\left(\frac{1-8t}{4\sqrt{t}}\right)\right]^2\right\} \tag{3}$$

where the aperture phase error parameters in the E- and H-plane are correspondingly

$$s = \frac{B\left(B-b\right)}{8\lambda P} \text{ and } t = \frac{A\left(A-a\right)}{8\lambda P} \tag{4}$$

and $C(\cdot)$ and $S(.)$ are the cosine and sine Fresnel integrals, respectively [26]. It has to be noticed that comparisons with measured data have shown that the maximum possible error of (1) is about $\pm 0.3\,\mathrm{dB}$ with 99% confidence limits [16, 27].

3. THE OPTIMAL PYRAMIDAL HORN DESIGN CRITERION

Obviously, see Figure 1, the lateral surface area of the horn is twice the sum of the areas of two trapezoids with heights $\sqrt{P^2+[(B-b)/2]^2}$ and $\sqrt{P^2+[(A-a)/2]^2}$ and bases a, A and b, B, respectively, i.e., it is

$$E=\frac{1}{2}\left[(a+A)\sqrt{4P^2+(B-b)^2}+(b+B)\sqrt{4P^2+(A-a)^2}\right] \quad (5)$$

Using (4) we also get:

$$B=\frac{b+\sqrt{b^2+32\lambda sP}}{2} \quad (6)$$

$$A=\frac{a+\sqrt{a^2+32\lambda tP}}{2} \quad (7)$$

Substitution of (6) and (7) into (5) gives E as a function of s, t, and P. It easily comes that

$$E=\frac{1}{2}\left[\begin{array}{l}\left(3a+\frac{\sqrt{t}}{q}\sqrt{P+\frac{q^2a^2}{t}}\right)\sqrt{P^2+\frac{s}{16q^2}P+\frac{b}{8q}\left(qb-\sqrt{s}\sqrt{P+\frac{q^2b^2}{s}}\right)}\\+\left(3b+\frac{\sqrt{s}}{q}\sqrt{P+\frac{q^2b^2}{s}}\right)\sqrt{P^2+\frac{t}{16q^2}P+\frac{a}{8q}\left(qa-\sqrt{t}\sqrt{P+\frac{q^2a^2}{t}}\right)}\end{array}\right] \quad (8)$$

with $q=(32\lambda)^{-1/2}$. The algebraic manipulation of (1), (6) and (7) gives that P is a root of

$$ab-\frac{\pi D}{2\,(8q)^4\,R_ER_H}+\frac{a\sqrt{s}}{q}\sqrt{P+\frac{q^2b^2}{s}}+\frac{b\sqrt{t}}{q}\sqrt{P+\frac{q^2a^2}{t}}+\frac{\sqrt{st}}{q^2}\sqrt{P^2+q^2\left(\frac{a^2}{t}+\frac{b^2}{s}\right)P+\frac{q^4a^2b^2}{st}}=0 \quad (9)$$

For the sake of notation simplicity, we set $\mathbf{x}=(s,t)$ and denote the right term of (8) as $F(\mathbf{x},P)$ and the left term of (9) as $U(\mathbf{x}, P)$. Therefore, the MLSA horn's design criterion is an optimization problem defined as:

$$\begin{aligned} &\text{find } \mathbf{x} : \min_{\mathbf{x}} F(\mathbf{x}, P) \\ &\text{given } U(\mathbf{x}, P) = 0 \end{aligned} \tag{10}$$

This problem can not be solved in closed form; its solution is obtained heuristically or by using an evolutionary optimization technique such as differential evolution, particle swarm optimization, genetic algorithms, artificial neural networks, etc. [28–45]. Further discussion of this issue is beyond the scope of the paper; in the examples presented here, we used a trial and error process to obtain the optimal solutions.

Next, we present the optimal values of the aperture phase error parameters of pyramidal horns in the area of practical interest. The horns operate in the range of 1 to 60 GHz; their directivity varies between 10 and 30 dB. Table 1 gives a list of the waveguides that we use in the design examples accompanied with their inner dimensions and recommended operation frequency range.

Table 1. Recommended operation frequency range and inner dimensions of common standard rectangular feed waveguides [12, 46].

ID	Name	Frequency range (GHz)	Inner dimensions	
			a (cm)	b (cm)
1	WR-770	0.96–1.45	19.558	9.779
2	WR-650	1.12–1.70	16.510	8.255
3	WR-430	1.70–2.60	10.922	5.461
4	WR-284	2.60–3.95	7.214	3.404
5	WR-229	3.30–4.90	5.817	2.908
6	WR-187	3.95–5.85	4.755	2.215
7	WR-137	5.85–8.20	3.485	1.580
8	WR-112	7.05–10.0	2.850	1.262
9	WR-90	8.20–12.4	2.286	1.016
10	WR-62	12.4–18.0	1.580	0.790
11	WR-42	18.0–26.5	1.067	0.432
12	WR-28	26.5–40.0	0.711	0.356
13	WR-22	33.0–50.5	0.569	0.284
14	WR-19	40.0–60.0	0.478	0.239
15	WR-15	50.0–75.0	0.376	0.188

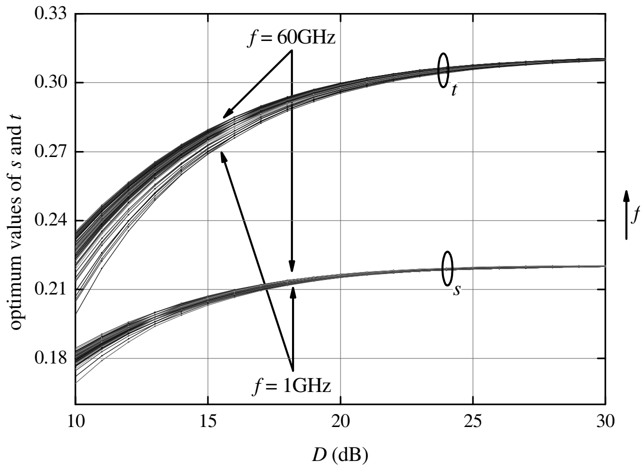

Figure 2. Optimal values for s and t versus directivity at $f = 1, 2, \ldots, 60\,\mathrm{GHz}$.

Figure 2 shows the optimal s and t as a function of directivity (in dB) for frequencies that range from 1 to 60 GHz with step $f_s = 1\,\mathrm{GHz}$. Notice that both optimal parameters increase exponentially with directivity and depend on frequency. In both cases, the impact of f decreases with directivity; moreover, the curves approach asymptotically at great frequency values.

We notice that optimal s (optimal t) varies between 0.17 (0.2) and 0.185 (0.235) at low values of directivity and reach the value 0.22 (0.31) at great D. In any case, the calculated optima are significantly different than those suggested by previous criteria (the optimal s and t values are $(s, t) = \{0.25, 0.375\}$ [1] and $(s, t) = \{0.26, 0.4\}$ [2], for example). At this point, it has to be mentioned that "any optimum design depends on the requirements" [2]. In the optimum gain horn, the requirement is the maximization of directivity for a given throat-to-aperture length. On the other hand, in the optimum design criterion discussed in [2] the requirement is the maximization of the quadratic phase error loss. Both criteria are related to the directivity of the horn, i.e., its radiation characteristics. In practice, these methods consider both the geometry of the horn and its radiation pattern characteristics. The proposed criterion considers only the geometrical parameters of the horn resulting in different optimal values of s and t.

Next, in Figures 3 and 4 we show the variation of optimal s and t, respectively, with f for different D. The directivity varies from 10 to 30 dB with step one decibel.

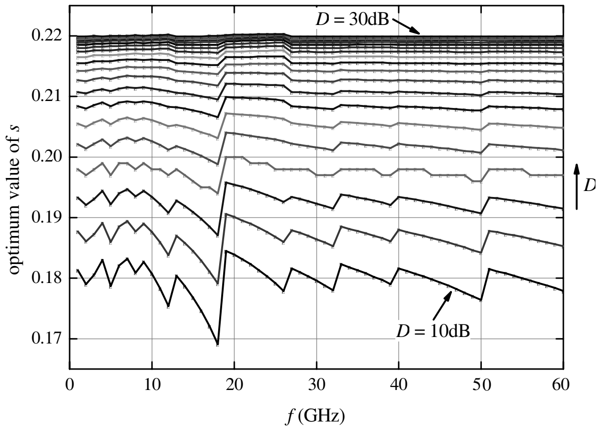

Figure 3. Optimal values for s versus frequency at $D = 10, 11, \ldots, 30\,\mathrm{dB}$.

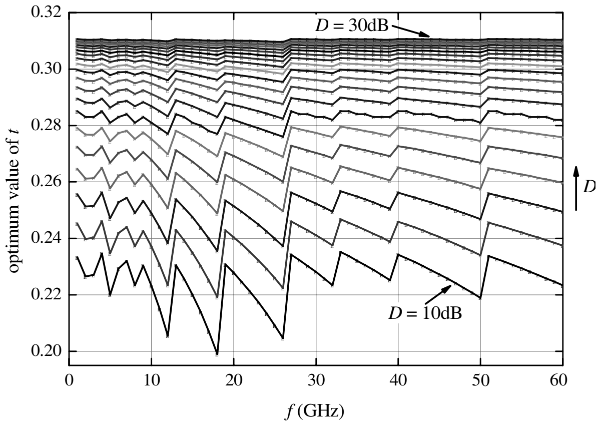

Figure 4. Optimal values for t versus frequency at $D = 10, 11, \ldots, 30\,\mathrm{dB}$.

Notice the small fluctuation of the optima around a mean value which depends on directivity. In practice, optimal s and t values decrease with frequency when a specific waveguide feeds the horn; however, their values increase when the waveguide is replaced with another one that has smaller inner dimensions. As it has already been mentioned, the impact of frequency decreases with directivity. We also notice that the curves approach asymptotically at great directivity values.

4. DESIGN APPROXIMATIONS

In the previous Section, we presented a set of curves which show that we can easily calculate the accurate optimal s and t values only at great D. Here, we present two approximate methods that estimate the optima s and t with increased accuracy. First, we approximate the curves in Figure 2 using least squares curve fitting [47, 48] (curve fitting is usually employed in the solution of engineering problems that cannot be solved analytically, e.g., [23, 49–57]). In order to get the best fit, we use the R^2 goodness-of-fit statistics metric. The fit improves as R^2 values approach unity. Figure 2 shows that the optimal s and t curves can be approximated as

$$s_i \approx \alpha_i - \beta_i \exp\left(-\gamma_i D\right), \quad i = 1, 2, \ldots, 60 \tag{11}$$

$$t_i \approx \kappa_i - \mu_i \exp\left(-\nu_i D\right), \quad i = 1, 2, \ldots, 60 \tag{12}$$

where D is measured in dB and ranges from 10 to 30 dB. The index i refers to the operation frequency (in GHz). Figure 5 illustrates values of the fitting coefficients (α_i and κ_i are omitted because they are practically independent of f); their numeric values are listed in Tables 2 and 3.

The factors γ_i and ν_i are close to each other and vary in a similar way. On the other hand, β_i and μ_i differ significantly; in fact, the local maxima of β_i appear to the same frequencies with the local minima of μ_i and vice-versa. Notice also the similarities between this figure and Figures 3 and 4.

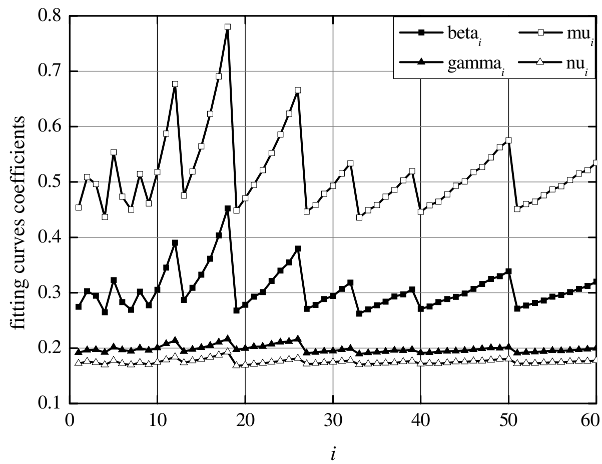

Figure 5. Coefficients of the fitting curves.

Table 2. Coefficients of the fitting curves of (11).

i	α_i	β_i	γ_i	i	α_i	β_i	γ_i
1	0.22113	0.27439	0.19170	31	0.22111	0.30693	0.19704
2	0.22114	0.30292	0.19619	32	0.22108	0.31828	0.19900
3	0.22120	0.29456	0.19689	33	0.22119	0.26238	0.18941
4	0.22117	0.26471	0.19223	34	0.22116	0.27009	0.19119
5	0.22120	0.32279	0.20160	35	0.22115	0.27724	0.19267
6	0.22117	0.28310	0.19670	36	0.22116	0.28389	0.19388
7	0.22125	0.26934	0.19423	37	0.22112	0.29343	0.19593
8	0.22127	0.30193	0.19984	38	0.22118	0.29707	0.19560
9	0.22121	0.27717	0.19594	39	0.22115	0.30604	0.19711
10	0.22125	0.30507	0.20052	40	0.22113	0.27087	0.19114
11	0.22119	0.34520	0.20762	41	0.22114	0.27525	0.19172
12	0.22118	0.39022	0.21356	42	0.22110	0.28317	0.19357
13	0.22111	0.28667	0.19400	43	0.22110	0.28829	0.19440
14	0.22111	0.30872	0.19738	44	0.22115	0.29265	0.19442
15	0.22111	0.33264	0.20064	45	0.22115	0.29884	0.19544
16	0.22109	0.36147	0.20429	46	0.22112	0.30704	0.19706
17	0.22101	0.40343	0.21050	47	0.22108	0.31567	0.19864
18	0.22093	0.45207	0.21638	48	0.22106	0.32469	0.20022
19	0.22131	0.26805	0.19709	49	0.22112	0.32972	0.20012
20	0.22132	0.27806	0.19912	50	0.22109	0.33874	0.20166
21	0.22129	0.29281	0.20238	51	0.22116	0.27112	0.19081
22	0.22140	0.30093	0.20272	52	0.22112	0.27683	0.19218
23	0.22135	0.32112	0.20691	53	0.22111	0.28156	0.19312
24	0.22131	0.34021	0.21046	54	0.22111	0.28602	0.19386
25	0.22140	0.35490	0.21180	55	0.22108	0.29312	0.19544
26	0.22134	0.37955	0.21587	56	0.22114	0.29592	0.19513
27	0.22112	0.27069	0.19102	57	0.22113	0.30117	0.19602
28	0.22113	0.27771	0.19223	58	0.22112	0.30704	0.19706
29	0.22110	0.28829	0.19440	59	0.22109	0.31228	0.19795
30	0.22115	0.29433	0.19448	60	0.22106	0.32004	0.19944

Finally, Table 4 gives the calculated R^2 values for the best fit approximation of each fitting curve. In the same table, we also present the corresponding F-statistic values [47, 48] (these values go toward infinity as the fit becomes more ideal). The listed data show that (11) and (12) adequately describe the optimal s and t values in the specific range of directivity and frequency.

Next, we propose two approximate methods for the calculation of the optimal s and t values at any given directivity and frequency

Table 3. Coefficients of the fitting curves of (12).

i	κ_i	μ_i	ν_i	i	κ_i	μ_i	ν_i
1	0.31375	0.45401	0.17204	31	0.31353	0.51524	0.17629
2	0.31360	0.50869	0.17564	32	0.31350	0.53384	0.17726
3	0.31358	0.49638	0.17391	33	0.31381	0.43573	0.17019
4	0.31376	0.43686	0.16973	34	0.31375	0.44878	0.17136
5	0.31335	0.55389	0.17746	35	0.31377	0.45842	0.17160
6	0.31360	0.47336	0.17167	36	0.31367	0.47372	0.17306
7	0.31369	0.45033	0.16973	37	0.31368	0.48531	0.17350
8	0.31351	0.51469	0.17356	38	0.31354	0.50292	0.17519
9	0.31367	0.46145	0.17019	39	0.31347	0.51954	0.17647
10	0.31347	0.51781	0.17401	40	0.31377	0.44601	0.17134
11	0.31322	0.58762	0.17845	41	0.31373	0.45797	0.17242
12	0.31286	0.67709	0.18396	42	0.31377	0.46444	0.17229
13	0.31369	0.47543	0.17338	43	0.31369	0.47771	0.17352
14	0.31347	0.51904	0.17682	44	0.31358	0.49306	0.17504
15	0.31338	0.56443	0.17937	45	0.31364	0.50112	0.17499
16	0.31315	0.62316	0.18331	46	0.31349	0.51768	0.17663
17	0.31293	0.69046	0.18724	47	0.31353	0.52729	0.17673
18	0.31257	0.78035	0.19280	48	0.31347	0.54430	0.17814
19	0.31367	0.44853	0.16791	49	0.31333	0.56266	0.17977
20	0.31358	0.47063	0.16933	50	0.31333	0.57533	0.18016
21	0.31349	0.49495	0.17087	51	0.31375	0.45090	0.17187
22	0.31341	0.52133	0.17243	52	0.31371	0.46000	0.17263
23	0.31325	0.55202	0.17449	53	0.31376	0.46468	0.17237
24	0.31311	0.58576	0.17663	54	0.31367	0.47587	0.17349
25	0.31297	0.62337	0.17896	55	0.31363	0.48646	0.17443
26	0.31277	0.66579	0.18150	56	0.31366	0.49241	0.17431
27	0.31378	0.44645	0.17147	57	0.31362	0.50329	0.17520
28	0.31381	0.45838	0.17177	58	0.31353	0.51524	0.17629
29	0.31367	0.47868	0.17376	59	0.31357	0.52127	0.17611
30	0.31366	0.49337	0.17438	60	0.31350	0.53459	0.17728

in the range 10–30 dB and 1–60 GHz, respectively. Obviously, if the operation frequency takes one of the discrete values in the range $\{1, 2, \ldots, 60\,\text{GHz}\}$, then we simply use (11) and (12) with the corresponding coefficients in Tables 2 and 3.

1st Method:

In this method, we calculate the optimal s and t using an interpolation technique [53, 58–60]. Let f_0 be the operation frequency.

Table 4. Goodness-of-fit values.

i	s-curves		t-curves		i	s-curves		t-curves	
	R^2	F-statistic	R^2	F-statistic		R^2	F-statistic	R^2	F-statistic
1	0.99939	3817790	0.99965	3124400	31	0.99950	4127450	0.99965	4021380
2	0.99944	3721700	0.99974	3625930	32	0.99959	4867410	0.99974	4583910
	0.99938	3664670	0.99976	3867920	33	0.99903	2525120	0.99976	2858980
4	0.99923	3302850	0.99961	2896700	34	0.99920	2989110	0.99961	3102820
5	0.99933	3061940	0.99984	5103560	35	0.99932	3455820	0.99984	3057730
6	0.99933	3631050	0.99969	3219610	36	0.99942	3926620	0.99969	3349090
7	0.99901	2609080	0.99967	3275720	37	0.99950	4468120	0.99967	3331810
8	0.99911	2561130	0.99976	3679460	38	0.99918	2634260	0.99976	3667770
9	0.99920	3152930	0.99967	3053290	39	0.99940	3461370	0.99967	4023910
10	0.99921	2881070	0.99978	3898940	40	0.99927	3245300	0.99978	3048140
11	0.99954	4396390	0.99988	6029160	41	0.99937	3684410	0.99988	2985460
12	0.99966	5355300	0.99996	14308000	42	0.99947	4341720	0.99996	3157920
13	0.99948	4303140	0.99968	3216890	43	0.99949	4354020	0.99968	3230810
14	0.99949	4025750	0.99976	3822510	44	0.99925	2877860	0.99976	3329920
15	0.99950	3798760	0.99984	4924670	45	0.99938	3436820	0.99984	3919990
16	0.99955	3813210	0.99991	7981210	46	0.99948	3975500	0.99991	3754920
17	0.99980	7869740	0.99995	11819700	47	0.99958	4854150	0.99995	4094110
18	0.99986	9971670	0.99998	31957200	48	0.99962	5152690	0.99998	4987800
19	0.99900	2761800	0.99969	3287690	49	0.99945	3479940	0.99969	4495830
20	0.99915	3156800	0.99971	3330470	50	0.99958	4454090	0.99971	5819790
21	0.99927	3549750	0.99977	3864920	51	0.99928	3254530	0.99977	3110150
22	0.99900	2442550	0.99980	4130980	52	0.99941	3948800	0.9998	2978950
23	0.99926	3157860	0.99984	4833300	53	0.99943	4034270	0.99984	3268410
24	0.99942	3844260	0.99988	6049140	54	0.99949	4401420	0.99988	3313120
25	0.99925	2818120	0.99993	8625080	55	0.99950	4417700	0.99993	3306580
26	0.99950	4011470	0.99995	12912400	65	0.99929	3026830	0.99995	3397400
27	0.99930	3375200	0.99963	3080050	57	0.99942	3629720	0.99963	4144530
28	0.99943	4013220	0.99965	3026370	58	0.99948	3975500	0.99965	4021380
29	0.99949	4354020	0.99969	3334410	59	0.99957	4742940	0.99969	3938540
30	0.99931	3099960	0.99972	3520660	60	0.99962	5244750	0.99972	4536180

In this case, the optimal s (we measure the directivity in dB) is

$$s \approx 0.2212 - \tilde{\beta} \exp\left(-\tilde{\gamma} D\right) \tag{13}$$

with

$$\begin{aligned} \tilde{\beta} &= k\beta_r + \bar{k}\beta_{r+1} \\ \tilde{\gamma} &= k\gamma_r + \bar{k}\gamma_{r+1} \end{aligned} \tag{14}$$

where r is the integer part of the ratio f_0/f_s. The coefficients k and $\bar{k}$ are

$$k = 1 - \left(\frac{f_0}{f_s} - r\right) \text{ and } \bar{k} = 1 - k \tag{15}$$

In practice, (13) is the linear combination of the two fitting curves defined at the frequencies which are closer to f_0. Similarly, the optimal t is calculated from the expression

$$t \approx 0.3135 - \tilde{\mu} \exp\left(-\tilde{\nu} D\right) \tag{16}$$

with

$$\begin{aligned} \tilde{\mu} &= k\mu_r + \bar{k}\mu_{r+1} \\ \tilde{\nu} &= k\nu_r + \bar{k}\nu_{r+1} \end{aligned} \tag{17}$$

2nd Method:

This method replaces the fitting coefficients in (11) and (12) with their mean values. The last are calculated from the data in Tables 2 and 3. In this case, the optimal aperture error phase parameters are (D is measured in dB)

$$s \approx 0.2212 - 0.3055 \exp\left(-0.1982 D\right) \tag{18}$$

and

$$t \approx 0.3135 - 0.5145 \exp\left(-0.1751 D\right) \tag{19}$$

In this case, substitution of (19) into (18) gives that in the optimal pyramidal horn it is

$$s \approx 0.2212 - 0.6482 \left(0.3135 - t\right)^{1.1319} \tag{20}$$

5. APPLICATION EXAMPLES AND DISCUSSION

In order to show the efficacy of our approach we give a series of examples. All the results were checked and verified with the antenna design software ORAMA [61].

First, we compare the geometric parameters of minimum surface area pyramidal horns with optimum directivity [1] ones. The design examples are taken from [12]. Table 5 gives the desired directivity, the operation frequency, the type of the feeding waveguide and the calculated aperture dimensions and throat-to-aperture length, see [12]. In the same table, we also give the lateral surface area E, the aperture area e and the volume of the rectangular parallelepiped V (for brevity, we will call it horn's volume) that encloses the horn (it is $e = AB$ and $V = eP$). Recall that the lateral surface area determines horn's weight while the next two parameters are related to the required installation space of the antenna.

Table 6 gives the horns' dimensions, geometric parameters and aperture phase error values for the design examples in Table 5 (columns 2–4) that are obtained from the proposed model. In our solution, we

Table 5. Design examples of optimum directivity pyramidal horns [12].

ID	D (dB)	f (GHz)	Waveguide	A (cm)	B (cm)	P (cm)	E (cm^2)	e (cm^2)	V (cm^3)
1	15.85	1.431	WR-650	57.362	43.867	37.259	5265.250	2516.299	93754.779
2	16.50	2.163	WR-430	40.889	31.442	29.448	2886.890	1285.632	37859.289
3	18.03	3.275	WR-284	32.252	24.967	29.385	2141.492	805.236	23661.851
4	19.95	4.968	WR-187	26.487	20.728	31.774	1804.389	549.023	17444.642
5	21.75	6.779	WR-137	23.855	18.806	36.601	1802.503	448.617	16419.836
6	22.70	10.340	WR-90	17.437	13.790	30.355	1075.022	240.456	7299.049
7	23.50	14.950	WR-62	13.185	10.503	25.419	676.541	138.482	3520.075
8	24.11	22.157	WR-42	9.572	7.586	20.044	380.907	72.613	1455.459
9	24.60	33.220	WR-28	6.730	5.377	14.950	200.228	36.187	540.999
10	25.45	49.480	WR-19	4.980	3.987	12.327	121.009	19.855	244.756

calculate the dimensions of the horns as in [62]. The data in Tables 5 and 6 show that the proposed criterion gives horns with smaller aperture sizes but greater throat-to-aperture length. The increase in P is justified from the decrease in the aperture area (in general, a pyramidal horn may have the same directivity with a larger aperture area one but it requires a greater axial length [1, 63]). The relative variation in the horns' dimensions, i.e., the ratio of the difference between the corresponding dimension of the proposed and the optimum gain horn to the value of the second one, is shown in Table 7. The reduction in A is greater than the reduction in B. In all the cases, the absolute relative variation values reduce with directivity; the reduction is greater for the axial length. Notice also, that both approximate methods give results very close to the ones obtained from the exact solution of (10).

Next, Table 8 gives the relative reduction in E, e, and V. As it was expected the proposed criterion produces horns with smaller lateral surface area. Moreover, we observe a significant reduction in e and V in each design example. The aperture area decreases due to the reduction in A and B. However, the reduction in V is smaller because the MLSA criterion gives horns with greater axial length (recall that $V = eP$).

Now let us compare our method with [2]. In that case, the design criterion related horn's optimality with a constant slant radius and variation of the aperture width in each principal plane by setting $s = 0.26$ and $t = 0.4$. Table 9 presents the calculated dimensions and the rest of the geometric parameters of interest for the design examples given in Table 5 (columns 2–4). Comparisons between the data in Tables 6 and 9 show that MLSA criterion gives horns with

Table 6. Optimal horn's parameters (MLSA criterion).

ID	s	t	A (cm)	B (cm)	P (cm)	E (cm^2)	e (cm^2)	V (cm^3)
Exact results								
1	0.2073	0.2805	52.619	41.827	40.416	5242.173	2200.895	88951.369
2	0.2091	0.2842	37.543	29.984	31.715	2867.082	1125.689	35701.237
3	0.2129	0.2912	29.666	23.835	31.235	2116.080	707.089	22085.928
4	0.2157	0.2977	24.416	19.791	33.403	1773.806	483.217	16140.899
5	0.2176	0.3019	22.023	17.962	38.225	1765.829	395.577	15120.936
6	0.2183	0.3036	16.110	13.172	31.624	1051.672	212.201	6710.642
7	0.2183	0.3053	12.195	10.024	26.432	661.160	122.243	3231.119
8	0.2192	0.3054	8.848	7.249	20.829	372.028	64.139	1335.954
9	0.2188	0.3067	6.228	5.132	15.518	195.458	31.962	495.988
10	0.2191	0.3075	4.610	3.806	12.782	118.037	17.546	224.269
Approximate results (method 1)								
1	0.2079	0.2830	52.767	41.843	40.336	5242.358	2207.930	89059.048
2	0.2094	0.2854	37.594	29.991	31.685	2867.104	1127.482	35724.256
3	0.2128	0.2920	29.696	23.826	31.222	2116.087	707.537	22090.717
4	0.2154	0.2974	24.410	19.781	33.416	1773.809	482.854	16135.056
5	0.2173	0.3023	22.036	17.950	38.224	1765.832	395.546	15119.358
6	0.2180	0.3034	16.107	13.166	31.634	1051.673	212.065	6708.457
7	0.2182	0.3052	12.194	10.023	26.435	661.160	122.220	3230.898
8	0.2189	0.3053	8.848	7.245	20.834	372.028	64.104	1335.538
9	0.2187	0.3069	6.230	5.131	15.518	195.459	31.966	496.050
10	0.2192	0.3077	4.611	3.806	12.779	118.037	17.549	224.265
Approximate results (method 2)								
1	0.2080	0.2814	52.664	41.869	40.372	5242.224	2204.989	89019.817
2	0.2096	0.2849	37.569	30.006	31.690	2867.097	1127.295	35723.992
3	0.2126	0.2916	29.684	23.819	31.234	2116.083	707.043	22083.787
4	0.2153	0.2979	24.426	19.775	33.409	1773.810	483.024	16137.354
5	0.2171	0.3021	22.032	17.945	38.233	1765.834	395.364	15115.961
6	0.2178	0.3038	16.116	13.159	31.631	1051.674	212.070	6708.000
7	0.2183	0.3051	12.192	10.025	26.435	661.160	122.225	3231.013
8	0.2186	0.3060	8.857	7.240	20.830	372.030	64.125	1335.717
9	0.2189	0.3066	6.228	5.132	15.518	195.458	31.962	495.988
10	0.2192	0.3075	4.610	3.806	12.781	118.037	17.546	224.251

significantly decreased (lateral surface and aperture) area and volume, see Table 10.

Next, we compare the MLSA horn's design criterion with [22]. The example 2 in [22] considered a C-band horn fed from WR-229 waveguide. The horn operated at 4.5 GHz and its desired directivity was 22 dB. Two design methods were suggested. In the first, the

Table 7. Comparison between the optimum directivity and the MLSA criterion: Relative variation of A, B and P (%).

ID	A			B			P		
	Exact	Approximate 1	Approximate 2	Exact	Approximate 1	Approximate 2	Exact	Approximate 1	Approximate 2
1	-8.27	-8.01	-8.19	-4.65	-4.61	-4.55	8.47	8.26	8.36
2	-8.18	-8.06	-8.12	-4.64	-4.61	-4.57	7.70	7.60	7.61
3	-8.02	-7.93	-7.96	-4.53	-4.57	-4.60	6.30	6.25	6.29
4	-7.82	-7.84	-7.78	-4.52	-4.57	-4.60	5.13	5.17	5.15
5	-7.68	-7.63	-7.64	-4.49	-4.55	-4.58	4.44	4.43	4.46
6	-7.61	-7.63	-7.58	-4.48	-4.53	-4.58	4.18	4.21	4.20
7	-7.51	-7.52	-7.53	-4.56	-4.57	-4.55	3.99	4.00	4.00
8	-7.56	-7.56	-7.47	-4.44	-4.50	-4.56	3.92	3.94	3.92
9	-7.46	-7.43	-7.46	-4.56	-4.58	-4.56	3.80	3.80	3.80
10	-7.43	-7.41	-7.43	-4.54	-4.54	-4.54	3.69	3.67	3.68

Table 8. Comparison between the optimum directivity and the MLSA criterion: Relative decrease of lateral surface area, aperture area and volume (%).

ID	Lateral surface area			Aperture area			Volume		
	Exact	Approximate 1	Approximate 2	Exact	Approximate 1	Approximate 2	Exact	Approximate 1	Approximate 2
1	0.44	0.43	0.44	12.53	12.25	12.37	5.12	5.01	5.05
2	0.69	0.69	0.69	12.44	12.30	12.32	5.70	5.64	5.64
3	1.19	1.19	1.19	12.19	12.13	12.19	6.66	6.64	6.67
4	1.69	1.69	1.69	11.99	12.05	12.02	7.47	7.51	7.49
5	2.03	2.03	2.03	11.82	11.83	11.87	7.91	7.92	7.94
6	2.17	2.17	2.17	11.75	11.81	11.81	8.06	8.09	8.10
7	2.27	2.27	2.27	11.73	11.74	11.74	8.21	8.22	8.21
8	2.33	2.33	2.33	11.67	11.72	11.69	8.21	8.24	8.23
9	2.38	2.38	2.38	11.68	11.66	11.68	8.32	8.31	8.32
10	2.46	2.46	2.46	11.63	11.61	11.63	8.37	8.37	8.38

calculated s and t parameters were 0.21 and 0.4, respectively; the optimal s and t values obtained from the second method were 0.257 and 0.44. The application of MLSA criterion gave $s = 0.2173$ and $t = 0.3021$. Table 11 lists the geometric parameters of the designed horns. Comparisons between our solution and the first design method in [22] shows that our proposal gives a horn with 4.19%, 9.49%, and 8.28%

Table 9. Optimal horns geometric parameters [2].

ID	A (cm)	B (cm)	P (cm)	E (cm^2)	e (cm^2)	V (cm^3)
1	60.131	45.624	39.126	5736.612	2743.417	107338.924
2	42.768	32.610	30.709	3119.579	1394.664	42828.752
3	33.590	25.760	30.246	2278.021	865.278	26171.210
4	27.484	21.288	32.349	1893.125	585.079	18926.733
5	24.695	19.259	37.014	1874.758	475.601	17603.896
6	18.036	14.106	30.617	1114.322	254.416	7789.449
7	13.630	10.735	25.595	699.625	146.318	3745.010
8	9.890	7.751	20.156	393.298	76.657	1545.106
9	6.952	5.491	15.023	206.513	38.173	573.479
10	5.142	4.070	12.371	124.596	20.928	258.900

Table 10. Comparison between [2] and the MLSA criterion: Relative decrease of lateral surface area, aperture area and volume (%).

ID	Lateral surface area	Aperture area	Volume
1	8.62	19.52	17.03
2	8.09	19.16	16.59
3	7.11	18.23	15.59
4	6.30	17.47	14.75
5	5.81	16.83	14.11
6	5.62	16.65	13.88
7	5.50	16.47	13.73
8	5.41	16.38	13.56
9	5.35	16.26	13.50
10	5.26	16.15	13.38

smaller lateral surface area, aperture area and volume, respectively. The MLSA criterion gives even better results when compared to the second design method in [22]; in this case, the reduction is 9.03%, 20.68%, and 18.99%, respectively.

A question that arises is whether or not we can apply the new method to design a horn that operates beyond 60 GHz. In this case, (10) gives an optimal solution because the optimization criterion does not impose any restrictions to the operation frequency. On the other hand, the first approximation design method can not be applied due to the absence of data for horns that operate at frequencies greater than 60 GHz. In the second method, the optimal s and t values depend

Table 11. Calculated horns' geometric parameters: [22] and MLSA criterion.

	s	t	A (cm)	B (cm)	P (cm)	E (cm^2)	e (cm^2)	V (cm^3)
Design 1, [22]	0.2100	0.4000	38.559	27.240	59.221	4535.222	1050.347	62202.609
Design 2, [22]	0.2570	0.4400	40.142	29.860	58.757	4776.341	1198.640	70428.498
MLSA criterion	0.2173	0.3021	34.128	27.857	60.009	4345.091	950.704	57050.778

Table 12. Calculated horns' geometric parameters: [1] and MLSA criterion.

	s	t	A(cm)	B(cm)	P(cm)	E(cm^2)	e(cm^2)	V(cm^3)
Optimum gain	0.25	0.375	2.324	1.855	4.813	22.364	4.311	20.749
MLSA criterion	0.2185	0.3061	2.145	1.766	4.973	21.674	3.788	18.838
Approximate method 2	0.2186	0.3058	2.144	1.767	4.974	21.678	3.788	18.844

only on D; however, the coefficients in (18) and (19) were derived from fitting curves that describe horns which operate at lower frequencies. In the following example, we will show that this approximate method can be extended to horns that operate beyond 60 GHz.

Let us consider a W-band horn with operation frequency 90 GHz and directivity 24 dB [64]. The input waveguide is WR-10; its inner dimensions are $a = 0.254$ cm and $b = 0.127$ cm [46]. Table 12 gives the geometric parameters of the optimum gain pyramidal horn (calculated as in [62]) and the horns designed with (10) and with the second approximate method. Again, our proposal gives horns with smaller E, e and V compared to the optimum gain design. We also notice that the second approximate method gives similar results to the exact solution. The validity of this approximate method is justified from the asymptotic behavior of the optimal s and t curves at high frequencies (see Figure 2).

Finally, it has to be mentioned that the weight of a horn depends on its lateral surface area but it is also related to the thickness of its walls and the material density. When the last two parameters do not vary in the horn body, the weight of the horn is proportional to its lateral surface area. In this case, MLSA criterion produces the lightest horn; the reduction of the horn's weight equals the reduction of the lateral surface area.

6. CONCLUSIONS

In this paper, we proposed the minimum lateral surface area (MLSA) criterion as an optimal pyramidal horn design criterion. According to this, the calculation of the optimal aperture phase error parameters and dimensions of a pyramidal horn is determined by the minimization of the horn's lateral surface area. The results were compared with the optimum gain horn and other well-known optimal horn's design criteria. In all the cases, the proposed criterion produced horns with smaller lateral surface area that is equivalent, under certain assumptions, to the production of lighter horns. Moreover, the aperture area and the required installation space of the horn are significantly reduced at an expense of marginal longer axial length. The MLSA criterion results in a constrained optimization problem that can not be solved analytically; for this reason, we further developed two simple approximate horn design methods. The obtained accuracy is adequate and allows their use in practical applications.

REFERENCES

1. Balanis, C. A., *Antenna Theory: Analysis and Design*, 3rd edition, John Wiley & Sons, Inc., Hoboken, 2005.
2. Milligan, T. A., *Modern Antenna Design*, 2nd edition, John Wiley & Sons, Inc., Hoboken, 2005.
3. Dehdasht-Heydari, R., H. R. Hassani, and A. R. Mallahzadeh, "Quad ridged horn antenna for UWB applications," *Progress In Electromagnetics Research*, Vol. 79, 23–38, 2008.
4. Mallahzadeh, A. R., A. A. Dastranj, and H. R. Hassani, "A novel dual-polarized double-ridged horn antenna for wideband applications," *Progress In Electromagnetics Research B*, Vol. 1, 67–80, 2008.
5. Green, H. E., "The phase centre of a pure mode, smooth wall, conical horn," *Progress In Electromagnetics Research B*, Vol. 4, 285–298, 2008.
6. Fazaelifar, M. and M. R. Fatorehchy, "Design, fabrication and test of parabolic cylinder reflector and horn for increasing the gain of vlasov antenna," *Progress In Electromagnetics Research Letters*, Vol. 4, 191–203, 2008.
7. Amineh, R. K., A. Trehan, and N. K. Nikolova, "TEM horn antenna for ultra-wide band microwave breast imaging," *Progress In Electromagnetics Research B*, Vol. 13, 59–74, 2009.
8. Mallahzadeh, A. R. and F. Karshenas, "Modified TEM horn an-

tenna for broadband applications," *Progress In Electromagnetics Research*, Vol. 90, 105–119, 2009.

9. Liu, Y. and S. Gong, "Design of a compact broadband double-ridged horn antenna," *Journal of Electromagnetic Waves and Applications*, Vol. 24, No. 5/6, 765–774, 2010.
10. Jacobs, B., J. W. Odendaal, and J. Joubert, "The effect of manufacturing and assembling tolerances on the performance of double-ridged horn antennas," *Journal of Electromagnetic Waves and Applications*, Vol. 24, No. 10, 1279–1290, 2010.
11. Güney, K., "Simple design method for optimum gain pyramidal horns," *AEU — International Journal of Electronics and Communications*, Vol. 55, 205–208, 2001.
12. Güney, K. and D. Karaboga, "New narrow aperture dimension expressions obtained by using a differential evolution algorithm for optimum gain pyramidal horns," *Journal of Electromagnetic Waves and Applications*, Vol. 18, No. 3, 321–339, 2004.
13. Güney, K. and N. Sarikaya, "Neural computation of wide aperture dimension of optimum gain pyramidal horn," *International Journal of Infrared and Millimeter Waves*, Vol. 26, 1043–1057, 2005.
14. Odendaal, J. W., J. Joubert, and M. J. Prinsloo, "Extended edge wave diffraction model for near-field directivity calculations of horn antennas," *IEEE Transactions on Instrumentation and Measurement*, Vol. 54, 2469–2473, 2005.
15. Akdagli, A. and K. Güney, "New wide-aperture-dimension formula obtained by using a particle swarm optimization for optimum gain pyramidal horns," *Microwave and Optical Technology Letters*, Vol. 48, 1201–1205, 2006.
16. Teo, J. L. and K. T. Selvan, "On the optimum pyramidal-horn design methods," *International Journal of RF and Microwave Computer-Aided Engineering*, Vol. 16, 561–564, 2006.
17. Najjar, Y., M. Moneer, and N. Dib, "Design of optimum gain pyramidal horn with improved formulas using particle swarm optimization," *International Journal of RF and Microwave Computer-Aided Engineering*, Vol. 17, 505–511, 2007.
18. Ikram, S. and G. Ahmad, "Design & implementation of a standard gain horn antenna for optimized gain and radiation pattern using MathCAD & HFSS," *Second International Conference on Electrical Engineering (ICEE 2008)*, Lahore, Pakistan, 2008, doi:10.1109/ICEE.2008.4553906.
19. Harima, K., M. Sakasai, and K. Fujii, "Determination of gain for

pyramidal-horn antenna on basis of phase center location," *2008 IEEE International Symposium on Electromagnetic Compatibility*, Detroit, USA, 2008, doi:10.1109/ISEMC.2008.4652010.

20. Baltzis, K. B., "Calculation of the half-power beamwidths of pyramidal horns with arbitrary gain and typical aperture phase error," *IEEE Antennas and Wireless Propagation Letters*, Vol. 9, 612–614, 2010.
21. Foged, L. J., A. Giacomini, L. Scialacqua, R. Morbidini, and N. Isman, "Comparative investigation of SGH performance prediction formulas, measurements and numerical modelling," *Fourth European Conference on Antennas and Propagation (EuCAP)*, 1–4, paper ID 924, Barcelona, Spain, 2010.
22. Milligan, T., "Scales for rectangular horns," *IEEE Antennas and Propagation Magazine*, Vol. 42, 79–83, 2000.
23. Kordas, G., K. B. Baltzis, G. S. Miaris, and J. N. Sahalos, "Pyramidal-horn design under constraints on half-power beamwidth," *IEEE Antennas and Propagation Magazine*, Vol. 44, 102–108, 2002.
24. Schelkunoff, S. A., *Electromagnetic Waves*, D. Van Nostrand Company, Inc., New York, 1943.
25. Aurand, J. F., "Pyramidal horns, Part II: a novel design method for horns of any desired gain and aperture phase error," *1989 IEEE Antennas Propagation Society International Symposium*, Vol. 3, 1439–1442, San Jose, USA, 1989.
26. Weisstein, E. W., *CRC Concise Encyclopedia of Mathematics*, 2nd edition, Chapman & Hall/CRC, Boca Raton, 2002.
27. Slayton, W. T., *Design and calibration of microwave antenna gain standards*, Rep. 4433, US Naval Research Laboratory, Washington DC, USA, 1954.
28. Baltzis, K. B. and K. Natsiouli, "A genetic algorithm based resource allocation scheme for throughput optimization of WCDMA networks," *International Review of Automatic Control*, Vol. 1, 125–131, 2008.
29. Stanković Z., B. Milovanović, and N. Donćov, "Hybrid empirical-neural model of loaded microwave cylindrical cavity," *Progress In Electromagnetics Research*, Vol. 83, 257–277, 2008.
30. Agastra, E., et al., "Genetic algorithm optimization of high-efficiency wide-band multimodal square horns for discrete lenses," *Progress In Electromagnetics Research*, Vol. 83, 335–352, 2008.
31. Rostami, A. and A. Yazdanpanah-Goharrizi, "Hybridization of neural networks and genetic algorithms for identification of

complex Bragg gratings," *Journal of Electromagnetic Waves and Applications*, Vol. 22, No. 5/6, 643–664, 2008.

32. Gürel, L. and Ö. Ergül, "Design and simulation of circular arrays of trapezoidal-tooth log-periodic antennas via genetic optimization," *Progress In Electromagnetics Research*, Vol. 85, 243–260, 2008.
33. Su, D. Y., D.-M. Fu, and D. Yu, "Genetic algorithms and method of moments for the design of pifas," *Progress In Electromagnetics Research Letters*, Vol. 1, 9–18, 2008.
34. Panduro, M. A., C. A. Brizuela, L. I. Balderas, and D. A. Acosta, "A comparison of genetic algorithms, particle swarm optimization and the differential evolution method for the design of scannable circular antenna arrays," *Progress In Electromagnetics Research B*, Vol. 13, 171–186, 2009.
35. Li, J.-Y. and J. L. Guo, "Optimization technique using differential evolution for yagi-uda antennas," *Journal of Electromagnetic Waves and Applications*, Vol. 23, No. 4, 449–461, 2009.
36. Pathak, N., G. K. Mahanti, S. K. Singh, J. K. Mishra, and A. Chakraborty, "Synthesis of thinned planar circular array antennas using modified particle swarm optimization," *Progress In Electromagnetics Research Letters*, Vol. 12, 87–97, 2009.
37. Mangoud, M. A. and H. M. Elragal, "Antenna array pattern synthesis and wide null control using enhanced particle swarm optimization," *Progress In Electromagnetics Research B*, Vol. 17, 1–14, 2009.
38. Li, J.-Y., "A bi-swarm optimizing strategy and its application of antenna design," *Journal of Electromagnetic Waves and Applications*, Vol. 23, 1877–1886, 2009.
39. Tokan, F. and F. Gunes, "The multi-objective optimization of non-uniform linear phased arrays using the genetic algorithm," *Progress In Electromagnetics Research B*, Vol. 17, 135–151, 2009.
40. Wang, A.-N. and W.-X. Zhang, "Design and optimization of broadband circularly polarized wide-slot antenna," *Journal of Electromagnetic Waves and Applications*, Vol. 23, No. 16, 2229–2236, 2009.
41. Goudos, S. K., Z. Zaharis, K. B. Baltzis, C. Hilas, and J. N. Sahalos, "A comparative study of particle swarm optimization and differential evolution on radar absorbing materials for EMC applications," *EMC Europe Workshop 2009 — Materials in EMC Applications*, 56–59, Athens, Greece, 2009, doi:10.1109/EMCEUROPE.2009.5189697.

42. Wang, W.-T., S.-X. Gong, Y.-J. Zhang, F.-T. Zha, J. Ling, and T. Wan, "Low RCS dipole array synthesis based on MoM-PSO hybrid algorithms," *Progress In Electromagnetics Research*, Vol. 94, 119–132, 2009.
43. Goudos, S. K., K. B. Baltzis, C. Bachtsevanidis, and J. N. Sahalos, "Cell-to-switch assignment in cellular networks using barebones particle swarm optimization," *IEICE Electronic Express*, Vol. 7, 254–260, 2010.
44. Vakula, D. and N. V. S. N. Sarma, "Using neural networks for fault detection in planar antenna arrays," *Progress In Electromagnetics Research Letters*, Vol. 14, 21–30, 2010.
45. Li, G., S. Yang, M. Huang, and Z. Nie, "Sidelobe suppression in time modulated linear arrays with unequal element spacing," *Journal of Electromagnetic Waves and Applications*, Vol. 24, No. 5/6, 775–783, 2010.
46. Pozar, D. M., *Microwave Engineering*, 3rd edition, John Wiley & Sons, Inc., Hoboken, 2005.
47. Hastie, T., R. Tibshirani, and J. Friedman, *The Elements of Statistical Learning: Data Mining, Inference, and Prediction*, 2nd Edition, Springer, New York, 2008.
48. Fox, J., *Applied Regression Analysis and Generalized Linear Models*, 2nd edition, Sage Publications, Inc., Los Angeles, 2008.
49. Wu, B., T. Su, B. Li, and C. H. Liang, "Design of tubular filter based on curve-fitting method," *Journal of Electromagnetic Waves and Applications*, Vol. 20, No. 8, 1071–1080, 2006.
50. Wang, Y. G., J. Wang, Z. Q. Zhao, and J. Y. Yang, "A novel method to calculate the phase center of antennas," *Journal of Electromagnetic Waves and Applications*, Vol. 22, No. 2/3, 239–250, 2008.
51. Li, Q., X. Lai, B. Wu, and T. Su, "Novel wideband coaxial filter with high selectivity in low rejection band," *Journal of Electromagnetic Waves and Applications*, Vol. 23, No. 8/9, 1155–1163, 2009.
52. Islam, M. T., M. Moniruzzaman, N. Misran, and M. N. Shakib, "Curve fitting based particle swarm optimization for UWB patch antenna," *Journal of Electromagnetic Waves and Applications*, Vol. 23, No. 17/18, 2421–2432, 2009.
53. Baltzis, K. B., "Empirical description of node-to-node distance density in non-overlapping wireless networks," *Journal of Microwaves, Optoelectronics and Electromagnetic Applications*, Vol. 9, 57–68, 2010.

54. Okabe, S., T. Tsuboi, G. Ueta, J. Takami, and H. Hirose, "Basic study of fitting method for base curve extraction in lightning impulse test techniques," *IEEE Transactions on Dielectrics and Electrical Insulation*, Vol. 17, 2–4, 2010.
55. Deschrijver, D. and T. Dhaene, "Rational fitting of S-parameter frequency samples with maximum absolute error control," *IEEE Microwave and Wireless Components. Letters*, Vol. 20, 247–249, 2010.
56. De Carlo, D. and S. Tringàli, "Automatic design of circular SIW resonators by a hybrid approach based on polynomial fitting and SVRMS," *Journal of Electromagnetic Waves and Applications*, Vol. 24, No. 5/6, 735–774, 2010.
57. Baltzis, K. B., "Polynomial-based evaluation of the impact of aperture phase taper on the gain of rectangular horns," *Journal of Electromagnetic Analysis and Applications*, Vol. 2, 424–430, 2010.
58. Philips, G. M., *Interpolation and Approximation by Polynomials*, Springer-Verlag Inc., New York, 2003.
59. Liu, X. F., Y. C. Jiao, F. S. Zhang, and Y. Wen, "Approximation method for reconstruction of 3-D antenna radiation patterns," *Journal of Electromagnetic Waves and Applications*, Vol. 21, No. 15, 2351–2358, 2007.
60. Yang, P., F. Yang, Z.-P. Nie, B. Li, and X. Tang, "Robust adaptive beamformer using interpolation technique for conformal antenna array," *Progress In Electromagnetics Research B*, Vol. 23, 215–228, 2010.
61. Sahalos, J. N., *Orthogonal Methods for Array Synthesis: Theory and the ORAMA Computer Tool*, John Wiley & Sons Ltd., Chichester, 2006.
62. Selvan, K. T., "Accurate design method for pyramidal horns of any desired gain and aperture phase error," *IEEE Antennas and Wireless Propagation Letters*, Vol. 7, 31–32, 2008.
63. Selvan, K. T., "Derivation of a condition for the normal gain behavior of pyramidal horns," *IEEE Transactions on Antennas Propagation*, Vol. 48, 1782–1784, 2000.
64. Aryshev, A., et al., "Development of microwave and soft X-ray sources based on coherent radiation and Thomson scattering," *Eighth International Symposium on Radiation from Relativistic Electrons in Periodic Structures*, Moscow, Russian Federation, 2009, doi:10.1088/1742-6596/236/1/012009.